15 Structural Neuroimaging

Stephanie J. Forkel and Marco Catani

Abstract

The field of neuroanatomy of language is moving forward at a fast pace. This advancement is partially due to developments in magnetic resonance imaging (MRI) and in particular MRI–based diffusion tractography, the latter allowing scientists to non-invasively study brain connections in the living brain. For the field of language studies this advancement is timely and important for two reasons. First, it liberates scientists from neuroanatomical models of language derived from animal studies. Second, it permits testing network correlates of linguistic models directly in the human brain. This chapter introduces general principles of MRI, diffusion MRI, and tractography (many technical terms will be explained in the Key Terms section; these are printed in italics on their first occurrence in the main text). An example of their applications will be used to explicate the versatility of this method in the realm of language studies, whilst discussing advantages and limitations of diffusion methods. Their non-invasiveness and wide availability will continue to provide new insights which will challenge our current understanding of the brain's language network.

Research Methods in Psycholinguistics and the Neurobiology of Language: A Practical Guide,
First Edition. Edited by Annette M. B. de Groot and Peter Hagoort.

Introduction

Structural imaging based on *computerized tomography* (CT) and *magnetic resonance imaging* (MRI) has progressively replaced traditional post-mortem studies in the process of identifying the neuroanatomical basis of language. In the clinical setting, the information provided by structural imaging has been used to confirm the exact diagnosis and formulate an individualized treatment plan. In the research arena, neuroimaging has permitted to understand neuroanatomy at the individual and group level. The possibility to obtain quantitative measures of lesions has improved correlation analyses between severity of symptoms, lesion load, and lesion location.

More recently, the development of structural imaging based on diffusion MRI has provided valid solutions to some of the major limitations of more conventional imaging. In stroke patients, diffusion can visualize early changes that are otherwise not detectable with more conventional structural imaging, with important implications for the clinical management of acute stroke patients. Beyond the sensitivity to early changes, diffusion imaging *tractography* presents the possibility of visualizing the trajectories of individual white matter pathways connecting distant regions. A pathway analysis based on tractography is offering a new perspective in neurolinguistics. First, it permits to formulate new anatomical models of language function in the healthy brain and allows to directly test these models in the human population without any reliance on animal models. Second, by defining the exact location of the damage to specific white matter connections we can understand the contribution of different mechanisms to the emergence of language deficits (e.g., cortical versus disconnection mechanisms). Finally, a better understanding of the anatomical variability of different language networks is helping to identify new anatomical predictors of language recovery. In this chapter we will focus on the principles of structural MRI and, in particular, diffusion imaging and tractography and present examples of how these methods have informed our understanding of variance in language performances in the healthy brain and language deficits in patient populations.

Assumptions and Rationale

In the last 30 years, advances in the field of structural imaging have primarily originated from a progressive improvement of *spatial resolution* of CT and MRI sequences, automatic methods for group-level analysis, and the development of diffusion imaging. Increased spatial resolution for structural images enabled scientists to obtain more precise quantitative measurements of cortical anatomy in the form of thickness, surface, and volume, and a better delineation of cortical and subcortical lesions. Diffusion imaging on the one hand is highly sensitive towards tissue damage and on the other hand allows to visualize and quantify white matter connections between cortical brain regions in the living human brain. When combined with automatic methods for tissue classification and group-level statistics, this has led to significant new insights on the anatomy of language. In addition, diffusion imaging has revealed tracts that are unique to the human brain and identified correlations

between lesions to specific tracts and severity of behavioral symptoms. In this paragraph we briefly discuss how these approaches are applied to study language in healthy volunteers and to patients with language deficits.

Structural Imaging Methods Based on Conventional MRI

Current algorithms for structural imaging analysis are able to differentiate neuronal tissue into gray matter, white matter, and *cerebrospinal fluid (CSF)* and extract quantitative measurements in single subjects and across large populations. These *brain morphometry* methods require an excellent *contrast* between different tissues (gray and white matter, CSF) to define gray matter density, gray matter volume, and the inner and outer surface of the cortex. Tissue classification improves with increasing spatial resolution of the imaging sequences.

Different automatic processing approaches to brain morphometry analysis have been developed and include voxel-based morphometry (VBM), deformation-based morphometry (DBM), and surface-based morphometry (SBM).

VBM is a fully automated technique that aims at estimating local differences in tissue composition, after minimizing gross anatomical differences between individuals (Ashburner & Friston, 2000). This is achieved by, first, estimating tissue classification based on *T1-weighted images*. Second, the *segmentation mask* (gray matter or white matter) is spatially linearly normalized to a *standard space* to assure that a specific *voxel* is at the same anatomical location across subjects. Third, to reduce the influence of inter-individual anatomical variability, *spatial smoothing* is applied. After correction for intensity non-uniformities, voxel intensities are measured and compared between groups or correlated with behavioral measurements (Ashburner & Friston, 2000). Finally, the results are corrected for multiple comparisons to avoid type I error (false positive results). With VBM it is possible to either analyze the entire brain or focus on specific regions of interest (Geva, Baron, Jones, Price, & Warburton, 2012; Leff *et al*., 2009; Rowan *et al*., 2007). In the healthy brain, VBM has been used on large datasets to understand structural characteristics of language–related areas. For example, Good *et al*. (2001) studied 465 healthy volunteers to show significant leftward asymmetry in Heschl's gyrus, frontal operculum, superior and inferior frontal sulci, and limbic structures. When combined with other measures, VBM aids exploring structural–functional relationships. Dorsaint-Pierre *et al*. (2006), for example, showed no correlation between language dominance (assessed with the Wada test) and asymmetry of gray matter concentration in posterior language areas (assessed with VBM) in epileptic patients. However, when more anterior language regions in the frontal lobe were analyzed, a significant correlation emerged.

Deformation Based Morphometry (DBM) has been developed as complementary method to VBM to partially overcome the limitations due to potential misregistration. In DBM non-linear *registration* algorithms are used to register the native image to a reference template and deformation field matrices are computed. The statistical analysis is then performed on the deformation matrices rather than on the registered voxels. In other words, DBM analyzes how much the voxel volumes change during image registration to the reference template, in contrast to VBM, which focuses on the residual image variability after its transformation. DBM is a preferred method

to investigate longitudinal changes, for example, in patients with progressive neurodegenerative disease (Brambati *et al*., 2015; Heim *et al*., 2014).

Finally, Surface Based Morphometry (SBM) offers the possibility of analyzing separate features of gray matter anatomy, such as surface area, cortical thickness, curvature, and volume. While thickness measures may provide some indication of underlying neuronal loss, reduced size of neuronal cell bodies, or degradation, surface area measures may reflect underlying white matter fibers (Van Essen, 1997). Similar to VBM, SBM requires a tissue segmentation of high-resolution T1-weighted images. However, in SBM the surface boundary between white and gray matter (inner boundary of cortex) and the boundary between gray matter and CSF (outer surface or pial surface) are calculated separately. The output file is a scalar value measured in millimeters, which indicates the distance between the inner and the outer surface for each vertex (Fischl & Dale, 2000). These techniques construct and analyze surfaces that represent structural boundaries between different tissues within the brain. As such, it differs from VBM and DBM approaches, which ultimately analyze image properties within the individual voxels. SBM is widely used in neurodevelopmental and neurodegenerative language disorders where the boundaries between cortex and white matter are preserved and reliable cortical measures of thickness, surface area and volume can be obtained (Ecker *et al*., 2016; Rogalski *et al*., 2011). In primary progressive aphasia (PPA) patients, for example, Rogalski *et al*., (2011) used DBM to investigate a specific correspondence between the pattern of cortical thinning and the language deficit profile. When applied to stroke patients, all automatic methods listed above have some shortfalls due to problems related to tissue classification and image normalisation, especially when lesions are large. Some authors have tried to overcome these limitations by developing dedicated lesion-based methods.

These lesion-based methods rely on the delineation of a lesion to estimate statistical associations between damaged tissue and behavioral deficits. Multiple algorithms are currently available to perform lesion-deficit analysis, including voxel-based lesion symptom mapping (VLSM) (Bates *et al*., 2003; see Chapter 16 for details), nonparametric mapping (NPM) (Rorden, Karnath, & Bonilha, 2007), and Anatomo-Clinical Overlapping Maps (AnaCOM) (Kinkingnéhun *et al*., 2007; see also Foulon *et al*., 2017). All these software packages differ with regard to their required input data (e.g., binary versus continuous scores), statistical analysis (parametric vs. nonparametric), underlying assumptions on voxel independence (e.g., single voxels analysis versus clusters of voxels analysis), and their need for different study designs (e.g., number and demographics of groups for comparison). Despite these differences, all lesion-deficit approaches need to fulfill prerequisites, including accurate and precise anatomical delineation of the lesions, neuropsychological assessments with high diagnostic sensitivity to the cognitive processes of interest, and reliable statistical methods to associate lesion characteristics with behavioral deficits (Medina, Kimberg, Chatterjee, & Coslett, 2010).

Diffusion-Weighted Imaging

Diffusion-weighted imaging (DWI) based on MRI was initially applied to the brain in the mid–1980s (Le Bihan *et al*., 1986) and its potential for studying stroke–related changes was promptly recognized (Moseley *et al*., 1990). The much later development of tractography algorithms (Mori *et al*., 1999; Conturo *et al*., 1999;

Basser *et al.*, 2000) made it possible to visualize white matter connections in the human brain and describe, for example, how language networks mature from childhood to adulthood and to characterize the effects of neurological and psychiatric disorders on the anatomy and function of language pathways.

Enthusiasm for the first tractography visualizations of white matter pathways was partially due to the resemblance of the *in vivo* virtual reconstructions to classical *post-mortem* dissections (Catani, Howard, Pajevic, & Jones, 2002; Lawes *et al.*, 2008). In addition, it became evident that tractography offered clear advantages compared to other invasive methods and could reveal new features of white matter anatomy that are unique to the human brain. For example, it became apparent that the arcuate fasciculus is a rather complex pathway formed by a direct long segment between the classical Broca's and Wernicke's regions and an indirect pathway passing via the inferior parietal lobule (i.e., Geschwind's region). The indirect pathway includes the anterior segment between Broca's and Geschwind's regions and the posterior segment between Wernicke's and Geschwind's regions (Catani, Jones, & ffytche, 2005). The availability of diffusion imaging in large groups of healthy volunteers permitted to replicate these findings and at the same time identify inter-individual differences. The three segments of the arcuate fasciculus are present in the left hemisphere in all healthy individuals, but in the right hemisphere the long segment shows great variability. Indeed, it is reported as being bilateral in 40% of the healthy population and extremely left lateralized in the remaining 60%, where this segment is either absent or very small in the right hemisphere (Catani *et al.*, 2007). These percentages change when females and males are analyzed separately, with a greater number of males showing an extreme left asymmetry. In recent years, tractography has been used to identify previously undescribed language pathways, such as the frontal aslant tract (FAT), which connects Broca's area to pre-supplementary motor cortex and medial prefrontal cortex (Catani *et al.*, 2013). When applied to language disorders, tractography provides diffusion indices that can be used to map white matter degeneration along specific tracts and reveal a direct association between the severity of tract damage and language deficits.

Apparatus and Nature of the Data

Current MRI scans allow to acquire structural T1- and T2-weighted images, FLAIR, perfusion and diffusion data in less than one hour. 1.5 or 3 Tesla MRI systems are typically used to acquire MR images by applying a *pulse sequence*, which contains radiofrequency (RF) pulses and gradient pulses with carefully controlled timings. There are various types of sequences, but they all have timing values, namely *echo time (TE)* and *repetition time (TR)*, both of which can be modified by the operator and influence the weighting, or sensitivity, of the image to specific tissues. MRI utilizes the natural properties of hydrogen atoms as part of water or lipids and the most important properties are the proton density (number of hydrogen atoms in a particular volume) and two characteristic relaxation times called longitudinal and transverse relaxation time, denoted as T1 and T2 respectively. Relaxation times describe how long the tissue takes to return to equilibrium after an RF pulse. Structural T1-weighted images are acquired using short TE/TR whereas *T2-weighted images* are acquired using long TE/TR (Figure 15.1). On T2-weighted images the signal from the cerebro-spinal

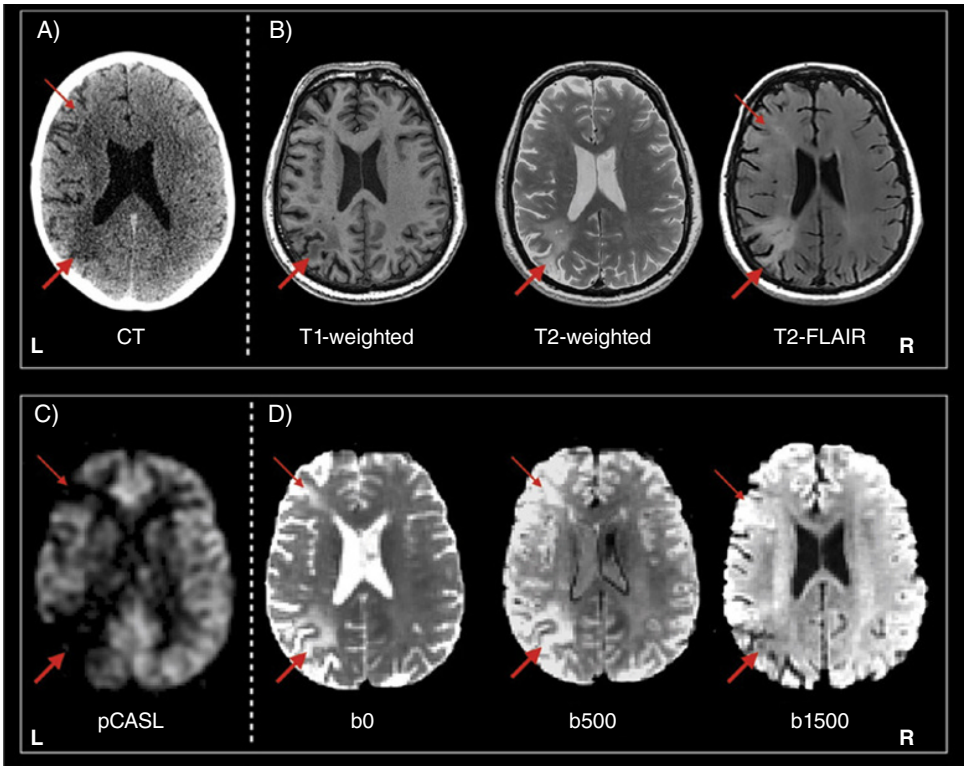

Figure 15.1 Imaging of an acute patient presenting with anomia following left inferior parietal and frontal lobe stroke.
A) Axial non-contrast computerized tomography (CT) scan demonstrates diffuse hypodensity in the parietal (indicated by thick red arrow) and frontal regions (indicated by thin red arrow), predominantly in white matter. The low signal-to-noise resolution and low white/gray matter boundary contrast of CT does not allow to determine the exact extent of the damage. B) T1- and T2-weighted and fluid-attenuated inverse recovery (FLAIR) images showing structural changes as hypo- and hyper-intense areas in the white matter, respectively. In structural T1-weighted images there is a clear contrast between white and gray matter, which is less evident in pathological T2-weighted images. In T2-weighted images the CSF signal is hyperintense (i.e., brighter) and gray matter appears brighter than white matter. Lesions appear hyperintense and may therefore be difficult to distinguish from CSF. In the FLAIR images there is a better contrast between the CSF (hypointense) and the lesion (hyperintense). C) Pulsed continuous Arterial Spin labelling (pCASL) perfusion-weighted MRI image of the lesion shows reduced cerebral blood flow (CBF) to a large area in the inferior parietal region and to a smaller area in the left frontal lobe. The degree of hypo-perfusion within the white matter is also noticeable but more difficult to distinguish from the CSF within the lateral ventricles. D) Series of diffusion images showing differences in the exact extension of the lesion depending on the b-value used to acquire them (non-diffusion weighted image: b=0 and diffusion-weighting: b=500 and b=1500). These images lack the spatial resolution of conventional MRI sequences but are sensitive to acute lesions within minutes. (*See insert for color representation of the figure.*)

fluid (CSF) in the ventricles and around the cortex is hyperintense and gray matter appears brighter than white matter. This poses a problem in stroke, as lesions appear hyperintense and may therefore be difficult to distinguish from CSF. To overcome this limitation a T2–weighted image with fluid–attenuated inversion recovery (FLAIR) is often acquired in clinical populations, where an additional inversion pulse is applied with the purpose of nulling signal from CSF. This renders CSF nearly fully suppressed and it appears dark, whilst lesions appear bright.

In clinical settings, T1- and T2-weighted images are widely used to characterize lesions due to tumors, traumatic brain injury, infection, neurodegeneration, and chronic stroke, but their sensitivity to acute ischemic changes is low.

Early changes in acute stroke can be best detected using perfusion- and diffusion-weighted imaging (Figure 15.1). Perfusion imaging is a method to measure *cerebral blood flow* (CBF) through the brain. Measurement of tissue perfusion depends on the ability to serially measure concentration of a tracer agent in the brain. These tracers are often exogenous contrast agents that are injected into the vascular system before acquiring the images. More recently less invasive sequences have been developed that use magnetic labeling of blood (endogenous) as the tracer (e.g., Arterial Spin Labelling, ASL) (Alsop & Detre, 1998). Perfusion imaging is a highly sensitive sequence to early ischaemic changes as it measures CBF, which if reduced for a critical time period, will cause irreversible damage (Figure 15.1). A mismatch between the lesion extent depicted on T1-weighted and perfusion images is often used to guide therapeutic decision as this mismatch is considered to quantify salvageable tissue at risk.

Diffusion MRI quantifies water diffusion in biological tissues. In neuronal tissue, the displacement of water molecules is not random due to the presence of biological structures such as cell membranes, filaments, and nuclei. These structures reduce diffusion distances in the three-dimensional space. In the white matter, the overall displacement is reduced unevenly (i.e., anisotropic) due to the presence of axonal membranes and *myelin* sheets, which restricts water diffusion in a direction perpendicular to the main orientation of the axonal fibers. Diffusion MRI can therefore detect diffusion drops in infarcted tissue within only several minutes of an arterial occlusion. Hereafter the signal stabilizes (pseudonormalization) before it progressively increases to become elevated in the chronic stage. For diffusion imaging, scanning times depend on various settings, including the b-value, which is a factor that reflects the strength and timing of the gradients used for the sequence: the higher the b-value, the stronger the diffusion effects in the data (Figure 15.1). At a given b-value, tissue with fast diffusion (e.g., CSF) experiences more signal loss, resulting in low intensity in the image, whilst tissue with slow diffusion (e.g., gray matter) produces high intensity in the image (Figure 15.1). Other important parameters are the number of gradient directions (ideally ≥30 for diffusion tensor studies, and ≥60 for *High Angular Resolution Diffusion Imaging; HARDI*) and the number of non-diffusion weighted images (Jones *et al*., 2002; Jones, 2008; Dell'Acqua *et al*., 2013). Non–diffusion weighted scans are of importance to better fit the diffusion metrics and to improve the correction of diffusion-weighted volumes for eddy current and motion artefacts. This is achieved by iterative alignment to the non-diffusion weighted volumes and to minimize T1 and T2 shine through effects (Le Bihan & Johansen-Berg, 2012). The rule of thumb is to acquire one non-diffusion weighted scan interleaved between diffusion-weighted volumes, usually with a 1:10 ratio.

Collecting and Analyzing Data

Raw data are collected as Digital Imaging and Communications in Medicine (DICOM) files from the scanner and converted to 4D Neuroimaging Informatics Technology Initiative (NIFTI) format, which can be readily imported in any standard neuroimaging program for visualization and further processing.

For diffusion imaging, in addition to the 4D image a *B*-matrix (which contains the gradient table that encodes the orientation of the gradients during the acquisition) is extracted to correctly preserve the orientational information by realigning the diffusion-weighted images to the reoriented *B*–matrix (Leemans & Jones, 2009). The *B*-matrix is usually provided by the analysis software during the initial processing steps. Prior to modeling, it is essential to perform manual quality control of the raw data (e.g., detecting missing volumes and misorientation of gradient tables) and automatic correction for artefacts (e.g., ghosting, wrapping, and ringing), head motion artefacts, and image distortions due to the scanner equipment and environment (e.g., eddy current, field inhomogeneity, echo planar imaging geometric distortion) (Jones, Knösche, & Turner, 2013). Once these steps have been implemented, tracking algorithms can be chosen to propagate the streamline reconstruction, using tensor or multi-fiber models and deterministic or probabilistic tracking. Virtual dissections of tractography datasets are used to obtain 3D reconstructions of pathways and tract-specific measurements along the tracts, such as volume and other diffusion indices calculated from the tensor or the fibre orientation distribution (FOD) (see below). The resulting average values per pathway and from each single subject can be submitted to statistical analysis. This allows to create percentage overlay maps for pathways of interest (Forkel, Thiebaut de Schotten, Kawadler *et al*., 2014b), establish group differences between controls and patients and between patients with different clinical presentations (Catani *et al*., 2013), detect volumetric left-right differences (Catani *et al*., 2007; Catani, Forkel, & Thiebaut de Schotten, 2010; Thiebaut de Schotten *et al*., 2011), and associate structural white matter anatomy with recovery from aphasia after stroke (Forkel, Thiebaut de Schotten, Dell'Acqua *et al*., 2014a).

Diffusion Tensor Imaging

The displacement of water molecules measured in a voxel can be described geometrically as an ellipsoid (the tensor) calculated from the diffusion coefficient values (eigenvalues, $\lambda_{1\text{-}3}$) and orientations (eigenvectors, $\nu_{1\text{-}3}$) of its three principal axes. A detailed analysis of the tensor can provide precise information about not only the average water molecular displacement within a voxel (e.g., *mean diffusivity*, *MD*), but also the degree of tissue anisotropy (e.g., *fractional anisotropy*, FA), and the main orientation of the underlying white matter pathways (e.g., principal eigenvector or color-coded maps). These indices provide complementary information about the microstructural composition and architecture of brain tissue.

Mean diffusivity (MD) is a rotational invariant quantitative index that describes the average mobility of water molecules and is calculated from the three eigenvalues ($\lambda1$, $\lambda2$, $\lambda3$) of the tensor ($MD = [(\lambda1 + \lambda2 + \lambda3)/3]$). Voxels containing gray and white matter tissue show similar MD values (Pierpaoli, Jezzard, Basser, Barnett, & Di Chiro,

1996). MD reduces with age within the first years of life and increases in those disorders characterized by demyelination, axonal injury, and edema (Beaulieu, 2009).

The fractional anisotropy (FA) index ranges from 0 to 1 and represents a quantitative measure of the degree of anisotropy in biological tissue. High FA values indicate a more anisotropic, that is, a non-equal, diffusion. In the healthy adult brain, FA varies from 0.2 (e.g., in gray matter) to ≥0.8 in the white matter. FA provides information about the organization of the tissue within a voxel (e.g., strongly or weakly anisotropic) and the microarchitecture of the fibers (e.g., parallel, crossing, kissing fibers). FA reduces in pathological tissue (e.g., demyelination, edema) and is therefore commonly used as an indirect index of microstructural organization.

Perpendicular [$(\lambda 2 + \lambda 3)/2$] and parallel diffusivity ($\lambda 1$) describe the diffusivity along the principal directions of the diffusion. The perpendicular diffusivity, also indicated with the term *radial diffusivity (RD)*, is generally considered a more sensitive index of axonal or myelin damage, although interpretation of changes in these indices in regions with crossing fibers is not always straightforward (Dell'Acqua & Catani, 2012). The principal eigenvector and color-coded maps are particularly useful to visualize the principal orientation of the tensor within each voxel (Pajevic & Pierpaoli, 1999).

Diffusion tractography, which is a family of algorithms able to propagate continuous *streamlines* from voxel to voxel, can be used to generate indirect measures of tract volume and microstructural properties along pathways. Tractography-derived inter-hemispheric differences in tract volume are widely reported in the literature, especially for language pathways (Catani *et al*., 2007).

In addition to tract volume, for each voxel intersected by streamlines, other diffusion indices can be extracted and a total average can be extrapolated from these. Examples of this application include tract-specific measurements of fractional anisotropy, mean diffusivity, parallel and radial diffusivity (Catani 2006). These can provide important information on the microstructural properties of streamlines and their organization. Asymmetry in FA, for example, could indicate differences in the axonal anatomy (intra-axonal composition, axon diameter, and membrane permeability), fiber myelination (myelin density, internodal distance, and myelin distribution), or fiber arrangement and morphology (axonal dispersion, axonal crossing, and axonal branching) (Beaulieu, 2002).

Other diffusion measurements may reveal more specific streamline properties. Changes in axial diffusivity, for example, could be related to intra-axonal composition, while RD may be more sensitive to changes in membrane permeability and myelin density (Song *et al*., 2002). These *in vivo* diffusion–based measurements allow connectional anatomy to be defined at different scales during development and in the adult brain.

Advanced Diffusion Models

One of the major limitations of the tensor model is the inability to estimate multiple fiber orientations. Several non-tensorial models have been proposed to overcome the limitations of the tensor model and the most commonly employed will be briefly mentioned below.

Multiparametric methods, for example, multitensor (Alexander, Barker, & Arridge, 2002; Tuch *et al.*, 2002) or "Ball and Stick" models (Behrens *et al.*, 2003) are model-dependent approaches in which the diffusion data are fitted with a chosen model that assumes a discrete number of fiber orientations (e.g., two or more). Nonparametric, model-independent methods such as diffusion spectrum imaging (DSI) (Wedeen, Hagmann, Tseng, Reese, & Weisskoff, 2005), q–Ball imaging (Tuch, Reese, Wiegell, & Van Wedeen, 2003), or diffusion orientation transform (Özarslan, Shepherd, Vemuri, Blackband, & Mareci, 2006) have been developed to better characterize the water displacement by using a spherical function or the diffusion orientation distribution function (dODF). Whilst tensor-based models only visualize one diffusion orientation per voxel, the multilobe shape of the dODF provides information on the number of fiber orientations, their orientation and the weight of each fiber component within a voxel.

A third group of methods takes advantage of both approaches by extracting directly the underlying fiber orientation (i.e., fiber-ODF) using a specific diffusion model for white matter fibers. The latter approaches are usually described as spherical deconvolution methods (Dell'Acqua, Simmons, Williams, & Catani, 2013) and they generally show higher angular resolution (i.e., the ability to resolve crossing fibers at smaller angles) compared with methods based on dODFs (Seunarine *et al.*, 2009; Catani *et al.*, 2012). Spherical deconvolution methods are becoming the methods of choice in an increasing number of studies as they require acquisition protocols that are close to clinical tractography protocols (e.g., a low number of diffusion gradient directions and b–values that are accessible on most clinical scanners).

Tractography Reconstructions

Deterministic and probabilistic tractography represent the most widely used approaches to perform 3D reconstructions of white matter trajectories using diffusion data. Compared to deterministic approaches in which the estimated fiber orientation (e.g., the direction of maximum diffusivity for the tensor model) is assumed to represent the best estimate to propagate streamlines, probabilistic methods generate multiple solutions to reflect also the variability or "uncertainty" of the estimated fiber orientation (Jbabdi & Johansen-Berg, 2011). These methods, therefore, provide additional information on the reproducibility of each tractography reconstruction by mapping the intrinsic uncertainty of individual diffusion datasets. The uncertainty quantified by probabilistic tractography is mainly driven by the magnetic resonance noise, partial volume effects, and inaccuracy of the chosen diffusion model. Therefore, the probability of individual maps should not be considered as a direct measure of the anatomical probability of the tract. Indeed, in some cases artefactual trajectories can have high probability similar to true anatomical pathways. Ultimately, in datasets without noise both deterministic and probabilistic approaches based on the same diffusion model would generate identical tractography maps. Understanding these basic assumptions underlying probabilistic tractography is important to correctly interpret the obtained results (Dell'Acqua & Catani, 2012).

Advanced diffusion models that resolve multiple white matter trajectories within a single voxel offer the possibility of describing tracts that are not visible using current diffusion tensor methods. This opens up the possibility to visualize and

describe tracts, which until now have been impossible to identify due to methodological limitations (Thiebaut de Schotten *et al.*, 2011; Catani *et al.*, 2012; Parlatini *et al.*, 2017). Although an exact knowledge of these fibers represents a significant step forward in our understanding of human anatomy, it is important to be aware that tractography based on advanced diffusion methods is prone to produce a higher number of false positives compared to the tensor model. Hence, validation of these tracts with complementary methods, such as intraoperative stimulation studies and postmortem staining (Elias, Zheng, Domer, Quigg, & Pouratian, 2012) is necessary before widely applying these anatomical models to clinical populations.

Atlasing

Until the advent of tractography, our knowledge of white matter anatomy was based on a small number of influential 19th and early 20th century post-mortem dissection atlases (Burdach, 1819; Déjerine, 1895; Sachs, 1892; Forkel *et al.*, 2015). In common with their contemporary counterparts (Talairach & Tournoux, 1988), these atlases emphasize the average anatomy of representative participants at the expense of variability between participants. In recent years, several research groups have used tractography to produce group atlases of the major white matter tracts (Catani & Thiebaut de Schotten, 2012; Hua *et al.*, 2008; Mori *et al.*, 2005; Rojkova *et al.*, 2016; Wakana *et al.*, 2007). By extracting the anatomical location of each tract from several participants, these atlases provide probability maps of each pathway and quantify their anatomical variability. These atlases help clinicians to establish a relationship of focal lesions with nearby tracts and improve clinical-anatomical correlation (Figure 15.2) (Thiebaut de Schotten *et al.*, 2014). It remains to be established, however, how much of this variability is due to a true underlying anatomical difference or the result of methodological limitations.

Tract Specific Measurements

Beyond visualizing white matter pathways, tractography facilitates quantitative analyses by extracting diffusion indices along the dissected tract. It is possible to characterize the microstructural properties of tissue in the normal and pathological brain and provide quantitative measurements for group comparisons or individual case studies (Figure 15.2) (Catani 2006).

The interpretation of these indices, however, is not always straightforward, especially in regions containing multiple fibers. An example of the complexity of this problem is the increase of fractional anisotropy commonly seen in the normal-appearing white matter regions distant to the lesioned area. Before interpreting these changes as indicative of "plasticity or remodeling," other explanations should be taken into account. In voxels containing both degenerating and healthy fibers, increases in fractional anisotropy values are, in fact, more likely due to the axonal degeneration of the perpendicular fibers (Wheeler-Kingshott & Cercignani, 2009; Dell'Acqua *et al.*, 2013). The lack of specificity of current diffusion indices (i.e., diffusion changes depend on a number of biological, biochemical, and microstructural factors) and the intrinsic voxel-specific rather than fiber-specific information

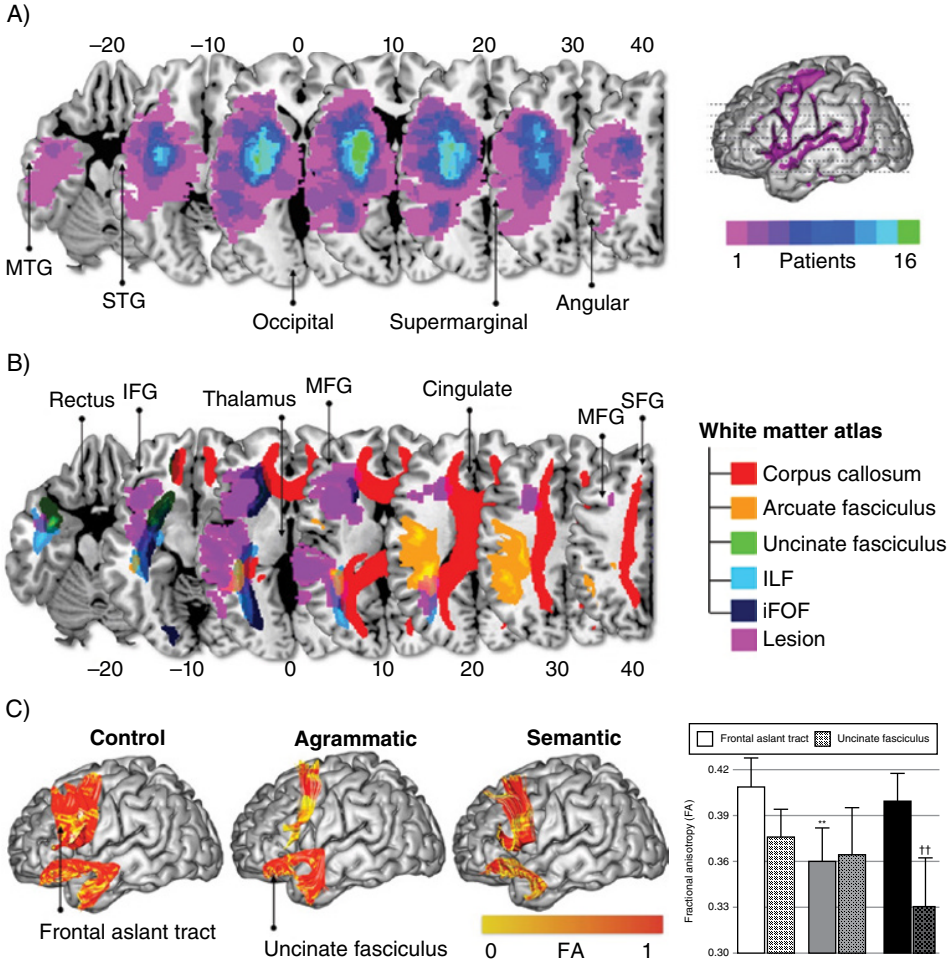

Figure 15.2 Lesion mapping based on T1-weighted data (A), on a diffusion tractography atlas (B), and an example of extracting tract–based measurements from tractography (C).
A) Group-level lesion overlay percentage maps for an aphasic stroke patient cohort (n=16) reconstructed on an axial template brain and projected onto the left lateral cortical surface. This method identifies areas most commonly affected by lesions within a group of patients. B) Lesion mask (purple) from a single stroke patient overlaid onto a tractography-based white matter atlas to extract measures of lesion load on pathways affected by the lesion. C) Differences in tract-specific measurements of the frontal aslant tract and uncinate fasciculus between control subjects and patients with non-fluent/agrammatic and semantic variants of primary progressive aphasia (PPA). Tractography reconstructions show the fractional anisotropy values mapped onto the streamlines of the frontal aslant tract and uncinate fasciculus of a control subject and two representative patients with PPA with non-fluent/agrammatic and semantic variant. Exemplary measurements of fractional anisotropy (FA) are reported for the frontal aslant tract (solid bars) and the uncinate fasciculus (patterned bars). **statistically significant different versus semantic group ($P < 0.05$), ††statistically significant different versus controls ($P < 0.001$). IFG: inferior frontal gyrus, MFG: middle frontal gyrus, SFG: superior frontal gyrus, MTG: middle temporal gyrus, STG: superior temporal gyrus. Source: Modified from Forkel *et al.*, 2014 and Catani *et al.*, 2013. (*See insert for color representation of the figure.*)

derived from current indices has stimulated scientists to work on new methods and novel diffusion indices. More recently, true tract-specific indices based on spherical deconvolution that better describe the microstructural diffusion changes of individual crossing fibers within the same voxel have been proposed. Changes in the *hindrance modulated orientation anisotropy* (*HMOA*) (Dell'Acqua *et al.*, 2013), for example, have a greater sensitivity than conventional fractional anisotropy values to detect degeneration that occurs only in one population of fibers, whereas the other crossing fibers remain intact. In the future, tractography combined with multimodal imaging methods will allow to extract even more specific tissue microstructure indices.

An Exemplary Study

In this section, we discuss how Forkel *et al.* (2014a) used conventional MRI in conjunction with diffusion tractography to identify anatomical predictors of language recovery after stroke. In this study, 18 patients with unilateral first-ever left hemisphere stroke and language impairment confirmed by the revised Western Aphasia Battery (WAB–R) (Kertesz, 2007) were prospectively recruited. Language and neuroimaging assessments were performed within two weeks after symptom onset and again after six months.

The 45-minute MRI scan included a high-resolution structural T1-weighted volume for lesion analyses and diffusion imaging data with 60 diffusion-weighted directions (b-value 1500 mm2/s) and seven interleaved non-diffusion weighted volumes. Matrix size was 128 × 128 × 60 and voxel size was 2.4 × 2.4 × 2.4 mm. Peripheral gating was applied to avoid brain pulsation artefacts. Diffusion tensor imaging data were preprocessed and corrected for eddy current and motion artefacts through iterative correction to the seven non-diffusion weighted volumes using ExploreDTI (www.exploreDTI.com). Whole brain tractography was performed from all brain voxels with fractional anisotropy >0.2. Streamlines were propagated with a step-size of 1 mm, using Euler integration and b-spline interpolation of the diffusion tensor field (Basser *et al.*, 2000). Where fractional anisotropy was <0.2 or when the angle between two consecutive tractography steps was >45°, streamline propagation was stopped.

Tractography dissections of the three segments of the arcuate fasciculus were obtained using a three regions of interest approach as previously described (Catani *et al.*, 2005). Regions of interest were defined on fractional anisotropy images in the patients' native space and included an inferior frontal region, an inferior parietal region, and a posterior temporal region. All streamlines passing through both frontal and temporal regions of interest were considered as belonging to the long segment of the arcuate fasciculus. All streamlines between temporal and parietal regions of interest were classified as posterior segment of the arcuate fasciculus and those between parietal and frontal regions of interest were labelled as anterior segment of the arcuate fasciculus. The volume for each segment was calculated as the number of voxels intersected by the streamlines of each segment. To control for the possibility that hemisphere size might be driving

the volume of the arcuate segments (i.e., larger hemisphere means larger arcuate fasciculus), the tract volume was normalized by the hemisphere volume (segment volume/hemisphere volume). The hemispheric volume was obtained using FMRIB Software Library package (FSL, http://www.fmrib.ox.ac.uk/fsl/). The normalized segment volume was then used for further analysis.

Stroke lesions were manually delineated on T1-weighted images and these delineations were saved as lesion masks. Their volume (number of voxels) was extracted using FSL and lesion masks were subsequently binarized (i.e., assigning a value of 0 or 1 to each voxel) and normalized to a standard space. Lesion masks were overlaid to create percentage maps to compute commonly damaged voxels. The average lesion size for this group was 21.62 cubic centimeters (standard deviation = 32.43 cubic centimeters). This number can be obtained by extracting the number of voxels within the lesion mask and multiplying these with the volume of the voxel in the underlying imaging scan. A standard neuroimaging software will provide this value automatically without the need for the calculation. An overlay of the patients' normalized lesions is shown in Figure 15.2A.

The aphasia quotient (AQ) was used as a measure of the patients' overall performance on the WAB-R at the acute stage and at follow-up. This measure was then inputted into a hierarchical regression analysis alongside demographic data (age, sex, education), lesion volume, and volume of the three segments. This analysis was run separately for the left and the right hemisphere. For the left hemisphere, adding tractography to the analysis did not significantly improve the predictive strength of longitudinal aphasia severity. By contrast, in the right hemisphere the addition of the normalized size of the long segment of the arcuate to a model based on age, sex, and lesion size, increased the predictive power of the variance at six months from nearly 30% to 57% (Figure 15.3). Of the four predictors only age and the right long segment were independent predictors. Gender and lesion size were marginally significant predictors.

These results indicate that the use of structural imaging based on lesion mapping and tractography can help clinicians identify trajectories of language recovery after stroke.

Advantages and Disadvantages of Diffusion Tractography

The ability of tracking connections in the living human brain allows to move above and beyond network models based on non-human primate tracing and small number of human post mortem studies. This is leading to the description of new tracts, some of which are important for language. In addition, fast acquisition sequences are now available to obtain high-quality data from patients who are prone to movement artefacts. When combining tractography with detailed linguistic assessment, neurobiological language models can be directly validated or falsified. However, despite a progressive amelioration of the spatial resolution of diffusion datasets, compared to classical axonal tracing studies, tractography is still unable to identify the smallest bundles and differentiate anterograde and retrograde connections. The level of noise in the diffusion data and the intrinsic MRI artefacts also constitute important factors

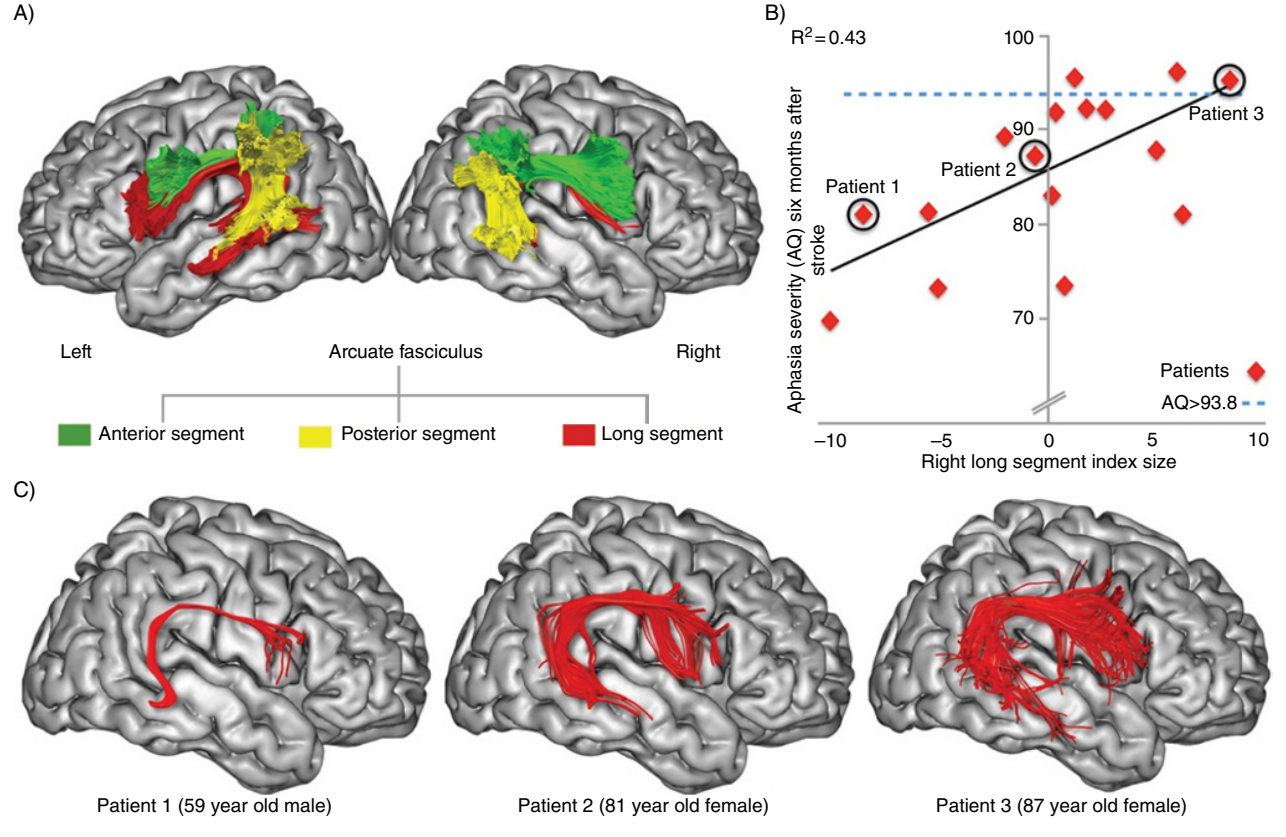

Figure 15.3 Anatomical variability in perisylvian white matter anatomy and its relation to post-stroke language recovery. A) shows the three segments of the arcuate fasciculus in the left and the right hemisphere obtained from a group average. B) shows a regression plot of the volume of the right long segment plotted against the six-month longitudinal aphasia quotient (AQ, corrected for age, sex, and lesion size). C) Indicates the right long segment for three exemplified patients (indicated in B) presenting with different degrees of language recovery at six months. Source: Modified from Forkel *et al.*, 2014. (*See insert for color representation of the figure.*)

that affect the precision and accuracy of the measurements and, as a consequence, the quality of the tractography reconstruction (Basser, Pajevic, Pierpaoli, Duda, & Aldroubi, 2000; Le Bihan, Poupon, Amadon, & Lethimonnier, 2006). Finally, diffusion tensor tractography assumes that fibers in each voxel are well described by a single orientation estimate, which is a valid assumption for voxels containing only one population of fibers with a similar orientation. The majority of white matter voxels, however, contain populations of fibers with multiple orientations. In these regions fibers cross, kiss, merge, or diverge, and the tensor model is inadequate to capture this anatomical complexity. More recent tractography developments based on HARDI methods and appropriate processing techniques are able to partially resolve fiber crossings. All these limitations may lead to tracking pathways that do not exist (false positive) or fail to track existing ones (false negative).

It is evident from all the considerations above that interpretation of tractography results requires experience and a priori anatomical knowledge. This is particularly true for the diseased brain, where alteration and anatomic distortion due to the presence of pathology generate tissue changes likely to lead to a greater number of artefactual reconstructions. Despite these limitations, tractography is the only technique that permits a quantitative assessment of white matter tracts in the living human brain. The recent development of MRI scanners with stronger gradients and multi-band acquisition sequences represents one of many steps towards a significant improvement of the diffusion tractography approach. The possibility of combining tractography with other imaging modalities will provide a complete picture of the functional anatomy of human language pathways.

Key Terms

Brain morphometry Measures brain structures based on structural MRI data. Techniques include voxel-based, surface-based, and deformation-based morphometry.

Cerebral blood flow (CBF) Blood supply to the brain in a given period of time. In an adult, CBF is typically 750 milliliters per minute or 15% of the cardiac output. This equates to an average perfusion of 50 to 54 milliliters of blood per 100 grams of brain tissue per minute.

Cerebrospinal fluid (CSF) Fluid surrounding the brain and spinal cord and filling the cavities inside the brain. It is produced within the ventricles of the brain and provides basic mechanical and immunological protection to the nervous system.

Computerized Tomography (CT) An imaging procedure that uses special x-ray equipment to create anatomical scans.

Contrast Various tissues have different signal intensities, or brightness, on MR images. The differences are described as the image, tissue, or signal contrast and allow to define boundaries between tissues, for example, gray-white matter.

Diffusion–weighted imaging (DWI) An advanced MRI pulse sequence based upon measuring the random Brownian motion of water molecules within the biological tissue contained in a voxel (3D volume).

Echo time (TE) Time between the radio frequency pulse and MR signal sampling, corresponding to maximum of echo.

Fractional Anisotropy (FA) A measure based on diffusion-weighted imaging describing the deviation from isotropy (equal diffusion in all directions) and measured between 0 (isotropic) and 1 (anisotropic). High FA is found in brain voxels with a minimal amount of crossing fibers.

High Angular Resolution Diffusion Imaging (HARDI) A "family" of advanced diffusion modeling methods that tries to overcome limitations of diffusion tensor imaging by resolving multiple fiber orientations. The main feature of HARDI approaches is to collect diffusion data along a large number of diffusion directions (≥60) to better characterize certain features of microstructure such as angular complexity.

Hindrance modulated orientation anisotropy (HMOA) Fiber specific diffusion index derived from spherical deconvolution analysis that provides information about white matter anisotropy and microstructure organization. Differently from more common voxel-based metrics (e.g., FA) that provide only a single average value per voxel, HMOA can have multiple values, one for each distinct fiber orientation resolved by spherical deconvolution.

Magnetic Resonance Imaging (MRI) Non-invasive imaging technique for obtaining anatomical images based on the magnetic properties of hydrogen atoms.

Mean Diffusivity (MD) A measure based on diffusion-weighted imaging describing the mean molecular motion, independent of tissue directionality.

Myelin: The myelin sheath is a lipid membrane wrapped around the nerve axons in a spiral fashion, which provides an electrically insulating layer. The myelin sheath originates from oligodendroglia cells in the central nervous system.

Pulse sequences A group of MRI sequences in which multiple radio frequency pulses are applied to produce a wide range of contrasts. The most frequent pulse sequences are spin echo, gradient echo, inversion recovery, susceptibility-weighted imaging, and diffusion.

Radial Diffusivity (RD) A DWI-based measure describing the diffusivity perpendicular to the axonal fibers, which is calculated from the mean magnitude of diffusion along two perpendicular directions that are orthogonal to the overall maximum diffusion direction.

Registration/normalization A neuroimaging registration method to spatially align a series of images, either from intra-subject or inter-subject image volumes, which is utilized in several steps of preprocessing.

Repetition time (TR) Time between two excitation pulses during an MRI acquisition.

Segmentation mask Partition of an image into a set of tissues that compose the image, including masks for gray and white matter, CSF, and lesioned tissue.

Spatial smoothing A process that requires convolving the data with a smoothing kernel in order to increase signal relative to noise, conform the data to a Gaussian field model, and to improve intersubject averaging.

Spatial resolution Spatial resolution of an image is determined by the size of the voxels. The smaller the size of the voxel, the higher the resolution and higher resolution allows to better segment tissues and identify lesions.

Standard space In order to compare brain scans they have to be aligned in a patient-orientation-independent space. Often this is achieved by using a reference template brain, a representative image with anatomical features in a coordinate space, which then provides a target to align individual images to.

Streamlines Tractography visualizes 3D reconstructions of the preferred orientation of water molecules, which is indicative of the underlying axonal structures. Given the inference, the term "streamlines" should be used in preference of axons or fibers when referring to tractography results.

T1-weighted image A basic pulse sequence (short TE/TR), which relies on the longitudinal relaxation after spins have been flipped into a transverse plane by a radiofrequency pulse.

T2-weighted image A basic pulse sequence (long TE/TR), which relies upon the transverse relaxation of the net magnetization vector.

Tractography A method used to reconstruct 3D trajectories of white matter pathways from diffusion data.

Voxel A 3D volume (a volume pixel), associated with a particular x-y-z coordinate in the brain, used in the analysis of 3D brain imaging data.

References

Alexander, D. C., Barker, G. J., & Arridge, S. R. (2002). Detection and modeling of non-Gaussian apparent diffusion coefficient profiles in human brain data. *Magnetic Resonance in Medicine*, *48*, 331–340. http://doi.org/10.1002/mrm.10209

Alsop, D. C., & Detre, J. A. (1998). Multisection cerebral blood flow MR imaging with continuous arterial spin labeling. *Radiology*, *208*, 410–416.

Ashburner, J., & Friston, K. J. (2000). Voxel-based morphometry—the methods. *NeuroImage*, *11*, 805–821.

Basser, P. J., Pajevic, S., Pierpaoli, C., Duda, J., & Aldroubi, A. (2000). In vivo fiber tractography using DT-MRI data. *Magnetic Resonance in Medicine*, *44*, 625–632.

Bates, E., Wilson, S. M., Saygin, A. P., Dick, F., Sereno, M. I., Knight, R. T., & Dronkers, N. F. (2003). Voxel-based lesion–symptom mapping. *Nature Neuroscience*, *6*, 448–450.

Beaulieu, C. (2002). The basis of anisotropic water diffusion in the nervous system – a technical review. *NMR in Biomedicine*, *15*, 435–455. http://doi.org/10.1002/nbm.782

Behrens, T. E. J., Woolrich, M. W., Jenkinson, M., Johansen-Berg, H., Nunes, R. G., Clare, S., *et al.* (2003). Characterization and propagation of uncertainty in diffusion-weighted MR imaging. *Magnetic Resonance in Medicine*, *50*, 1077–1088. http://doi.org/10.1002/mrm.10609

Brambati, S. M., Amici, S., Racine, C. A., Neuhaus, J., Miller, Z., Ogar, J., *et al.* (2015). Longitudinal gray matter contraction in three variants of primary progressive aphasia: A tenser-based morphometry study. *NeuroImage Clinical*, *8*, 345–355. http://doi.org/10.1016/j.nicl.2015.01.011

Burdach, C. F. (1819). Vom Baue und Leben des Gehirns. Leipzig: Dyk.

Catani, M. (2006). Diffusion tensor magnetic resonance imaging tractography in cognitive disorders. *Current Opinion in Neurology*, *19*, 599–606.

Catani, M., Allin, M. P. G., Husain, M., Pugliese, L., Mesulam, M. M., Murray, R. M., & Jones, D. (2007). Symmetries in human brain language pathways correlate with verbal recall. *Proceedings of the National Academy of Sciences of the United States of America*, *104*, 17163–17168. http://doi.org/10.1073/pnas.0702116104

Catani, M., Dell'Acqua, F., Vergani, F., Malik, F., Hodge, H., Roy, P., *et al.* (2012). Short frontal lobe connections of the human brain. *Cortex*, *48*, 273–291. http://doi.org/10.1016/j.cortex.2011.12.001

Catani, M., Forkel, S. J., & Thiebaut de Schotten, M. (2010). Asymmetry of the white matter pathways in the brain. In K. Hugdahl & R. Westerhausen (Eds.), *The two halves of the brain* (pp. 1–34). Cambridge (MA): MIT Press.

Catani, M., Howard, R. J., Pajevic, S., & Jones, D. (2002). Virtual in vivo interactive dissection of white matter fasciculi in the human brain. *NeuroImage*, *17*, 77–94. http://doi.org/10.1006/nimg.2002.1136

Catani, M., Jones, D., & ffytche, D. H. (2005). Perisylvian language networks of the human brain. *Annals of Neurology*, *57*, 8–16. http://doi.org/10.1002/ana.20319

Catani, M., Mesulam, M. M., Jakobsen, E., Malik, F., Martersteck, A., Wieneke, C., *et al.* (2013). A novel frontal pathway underlies verbal fluency in primary progressive aphasia. *Brain*, *136*, 2619–2628. http://doi.org/10.1093/brain/awt163

Catani, M., & Thiebaut de Schotten, M. (2008). A diffusion tensor imaging tractography atlas for virtual in vivo dissections. *Cortex*, *44*, 1105–1132. http://doi.org/10.1016/j.cortex.2008.05.004

Catani, M., & Thiebaut de Schotten, M. (2012). Atlas of human brain connections. Oxford: OUP Oxford.

Conturo, T. E., Lori, N. F., Cull, T. S., Akbudak, E., Snyder, A. Z., Shimony, J. S., *et al.* (1999). Tracking neuronal fiber pathways in the living human brain. *Proceedings of the National Academy of Sciences*, *96*, 10422–10427.

Déjerine, J. J. (1895). Anatomie des centres nerveux. Paris: Rueff at Cie.

Dell'Acqua, F., & Catani, M. (2012). Structural human brain networks: Hot topics in diffusion tractography. *Current Opinion in Neurology*, *25*, 375–383. http://doi.org/10.1097/WCO.0b013e328355d544

Dell'Acqua, F., Simmons, A., Williams, S. C. R., & Catani, M. (2013). Can spherical deconvolution provide more information than fiber orientations? Hindrance modulated orientational anisotropy, a true-tract specific index to characterize white matter diffusion. *Human Brain Mapping*, *34*, 2464–2483. http://doi.org/10.1002/hbm.22080

Dorsaint-Pierre, R., Penhune, V. B., Watkins, K. E., Neelin, P., Lerch, J. P., Bouffard, M., & Zatorre, R. J. (2006). Asymmetries of the planum temporale and Heschl's gyrus: Relationship to language lateralization. *Brain*, *129*, 1164–1176. http://doi.org/10.1093/brain/awl055

Ecker, C., Andrews, D., Dell'Acqua, F., Daly, E., Murphy, C., Catani, M., *et al.*; MRC AIMS Consortium. Murphy D. G. (2016). Relationship between cortical gyrification, white matter connectivity, and autism spectrum disorder. *Cerebral Cortex*, *26*, 3297–3309. doi: 10.1093/cercor/bhw098

Elias, W. J., Zheng, Z. A., Domer, P., Quigg, M., & Pouratian, N. (2012). Validation of connectivity-based thalamic segmentation with direct electrophysiologic recordings from human sensory thalamus. *NeuroImage*, *59*, 2025–2034. http://doi.org/10.1016/j.neuroimage.2011.10.049

Fischl, B., & Dale, A. M. (2000). Measuring the thickness of the human cerebral cortex from magnetic resonance images. *Proceedings of the National Academy of Sciences of the United States of America*, *97*, 11050–11055. http://doi.org/10.1073/pnas.200033797

Forkel, S. J., Mahmood, S., Vergani, F., & Catani, M. (2015). The white matter of the human cerebrum: part I The occipital lobe by Heinrich Sachs. *Cortex*, *62*, 182–202.

Forkel, S. J., Thiebaut de Schotten, M., Dell'Acqua, F., Kalra, L., Murphy, D. G. M., Williams, S. C. R., & Catani, M. (2014a). Anatomical predictors of aphasia recovery: A tractography study of bilateral perisylvian language networks. *Brain*, *137*(Pt 7), 2027–2039. http://doi.org/10.1093/brain/awu113

Forkel, S. J., Thiebaut de Schotten, M., Kawadler, J. M., Dell'Acqua, F., Danek, A., & Catani, M. (2014b). The anatomy of fronto-occipital connections from early blunt dissections to contemporary tractography. *Cortex*, *56*, 73–84. http://doi.org/10.1016/j.cortex.2012.09.005

Foulon, C., Cerliani, L., Kinkingnéhun, S., Levy, R., Rosso, C., Urbanski, M., *et al.* (2017). Advanced lesion symptom mapping analyses and implementation as BCBtoolkit. http://dx.doi.org/10.1101/133314

Geva, S., Baron, J.-C., Jones, P. S., Price, C. J., & Warburton, E. A. (2012). A comparison of VLSM and VBM in a cohort of patients with post-stroke aphasia. *NeuroImage Clinical*, *1*, 37–47. http://doi.org/10.1016/j.nicl.2012.08.003

Good, C. D., Johnsrude, I. S., Ashburner, J., Henson, R. N. A., Friston, K. J., & Frackowiak, R. S. J. (2001). A voxel-based morphometric study of ageing in 465 normal adult human brains. *NeuroImage*, *14*, 21–36. http://doi.org/10.1006/nimg.2001.0786

Heim, S., Pieperhoff, P., Grande, M., Kuijsten, W., Wellner, B., Sáez, L. E., *et al.* (2014). Longitudinal changes in brains of patients with fluent primary progressive aphasia. *Brain and Language*, *131*, 11–19. http://doi.org/10.1016/j.bandl.2013.05.012

Hua, K., Zhang, J., Wakana, S., Jiang, H., Li, X., Reich, D. S., *et al.* (2008). Tract probability maps in stereotaxic spaces: Analysis of white matter anatomy and tract-specific quantification. *NeuroImage*, *39*(1), 336–347.

Jbabdi, S., & Johansen-Berg, H. (2011). Tractography: Where do we go from here? *Brain Connectivity*, *1*, 169–183. http://doi.org/10.1089/brain.2011.0033

Jones, D. (2008). Studying connections in the living human brain with diffusion MRI. *Cortex*, *44*, 936–952.

Jones, D., Knösche, T. R., & Turner, R. (2013). White matter integrity, fiber count, and other fallacies: The do's and don'ts of diffusion MRI. *NeuroImage*, *73*, 239–254. http://doi.org/10.1016/j.neuroimage.2012.06.081

Jones, D. K., Williams, S. C. R., Gasston, D., Horsfield, M. A., Simmons, A., & Howard, R. (2002). Isotropic resolution diffusion tensor imaging with whole brain acquisition in a clinically acceptable time. *Human Brain Mapping*, *15*, 216–230.

Kertesz, A. (2007). Western Aphasia Battery – Revised. San Antonio: PsychCorp.

Kinkingnéhun, S., Volle, E., Pélégrini-Issac, M., Golmard, J.-L., Lehéricy, S., Boisgueheneuc, Du, F., *et al.* (2007). A novel approach to clinical–radiological correlations: Anatomo-Clinical Overlapping Maps (AnaCOM): Method and validation. *NeuroImage*, *37*, 1237–1249. http://doi.org/10.1016/j.neuroimage.2007.06.027

Lawes, N., Barrick, T. R., Murugam, V., Spierings, N., Evans, D. R., Song, M., & Clark, C. A. (2008). Atlas-based segmentation of white matter tracts of the human brain using diffusion tensor tractography and comparison with classical dissection. *NeuroImage*, *39*, 62–79. http://doi.org/10.1016/j.neuroimage.2007.06.041

Le Bihan, D., & Johansen-Berg, H. (2012). Diffusion MRI at 25: Exploring brain tissue structure and function. *NeuroImage*, *61*, 324–341. http://doi.org/10.1016/j.neuroimage.2011.11.006

Le Bihan, D., Breton, E., Lallemand, D., Grenier, P., Cabanis, E., & Laval-Jeantet, M. (1986). MR imaging of intravoxel incoherent motions: Application to diffusion and perfusion in neurologic disorders. *Radiology*, *161*, 401–407. http://doi.org/10.1148/radiology.161.2.3763909

Le Bihan, D., Poupon, C., Amadon, A., & Lethimonnier, F. (2006). Artifacts and pitfalls in diffusion MRI. *Journal of Magnetic Resonance Imaging*, *24*, 478–488. http://doi.org/10.1002/jmri.20683

Leemans, A., & Jones, D. (2009). The B-matrix must be rotated when correcting for subject motion in DTI data. *Magnetic Resonance in Medicine*, *61*, 1336–1349. http://doi.org/10.1002/mrm.21890

Leff, A. P., Schofield, T. M., Crinion, J. T., Seghier, M. L., Grogan, A., Green, D. W., & Price, C. J. (2009). The left superior temporal gyrus is a shared substrate for auditory short-term memory and speech comprehension: Evidence from 210 patients with stroke. *Brain*, *132*, 3401–3410. http://doi.org/10.1093/brain/awp273

Medina, J., Kimberg, D. Y., Chatterjee, A., & Coslett, H. B. (2010). Inappropriate usage of the Brunner-Munzel test in recent voxel-based lesion-symptom mapping studies. *Neuropsychologia*, *48*, 341–343. http://doi.org/10.1016/j.neuropsychologia.2009.09.016

Mori, S., Crain, B. J., Chacko, V. P., & Van Zijl, P. C. (1999). Three-dimensional tracking of axonal projections in the brain by magnetic resonance imaging. *Ann Neurol*, *45*, 265–269.

Mori, S., Wakana, S., van Zijl, P. C. M., & Nagae-Poetscher, L. M. (2005). MRI Atlas of Human White Matter. Amsterdam, The Netherlands: Elsevier.

Moseley, M. E., Kucharczyk, J., Mintorovitch, J., Cohen, Y., Kurhanewicz, J., Derugin, N., *et al.* (1990). Diffusion-weighted MR imaging of acute stroke: correlation with T2-weighted and magnetic susceptibility-enhanced MR imaging in cats. *American Journal of Neuroradiology*, *11*, 423–429.

Özarslan, E., Shepherd, T. M., Vemuri, B. C., Blackband, S. J., & Mareci, T. H. (2006). Resolution of complex tissue microarchitecture using the diffusion orientation transform (DOT). *NeuroImage*, *31*, 1086–1103. http://doi.org/10.1016/j.neuroimage.2006.01.024

Pajevic, S., & Pierpaoli, C. (1999). Color schemes to represent the orientation of anisotropic tissues from diffusion tensor data: Application to white matter fiber tract mapping in the human brain. *Magnetic Resonance in Medicine*, *42*, 526–540.

Pierpaoli, C., Jezzard, P., Basser, P. J., Barnett, A., & Di Chiro, G. (1996). Diffusion tensor MR imaging of the human brain. *Radiology*, *201*, 637–648. http://doi.org/10.1148/radiology.201.3.8939209

Rogalski, E., Cobia, D., Harrison, T. M., Wieneke, C., Thompson, C. K., Weintraub, S., & Mesulam, M.-M. (2011). Anatomy of language impairments in primary progressive aphasia. *The Journal of Neuroscience*, *31*, 3344–3350. http://doi.org/10.1523/JNEUROSCI.5544-10.2011

Rojkova, K., Volle, E., Urbanski, M., Humbert, F., Dell'Acqua, F., & Thiebaut de Schotten, M. (2016). Atlasing the frontal lobe connections and their variability due to age and education: A spherical deconvolution tractography study. *Brain Structure & Function*, *221*, 1751–1766. http://doi.org/10.1007/s00429-015-1001-3

Rorden, C., Karnath, H.-O., & Bonilha, L. (2007). Improving lesion-symptom mapping. *Journal of Cognitive Neuroscience*, *19*, 1081–1088.

Rowan, A., Vargha-Khadem, F., Calamante, F., Tournier, J.-D., Kirkham, F. J., Chong, W. K., *et al.* (2007). Cortical abnormalities and language function in young patients with basal ganglia stroke. *NeuroImage*, *36*, 431–440. http://doi.org/10.1016/j.neuroimage.2007.02.051

Sachs, H. (1892). Das Hemisphaerenmark des menschlichen Grosshirns. I. Der Hinterhauptlappen. Leipzig: Georg Thieme Verlag.

Song, S. K., Sun, S. W., Ramsbottom, M. J., Chang, C., Russell, J., & Cross, A. H. (2002). Dysmyelination revealed through MRI as increased radial (but unchanged axial) diffusion of water. *Neuroimage*, *17*, 1429–1436.

Seunarine, K. K. & Alexander, D. C. (2009). Multiple Fibers: Beyond the Diffusion Tensor. In H. Johansen-Berg & TEJ Behrens (Eds.), *Diffusion MRI: From quantitative measurement to in-vivo neuroanatomy* (pp. 55–72). Oxford: Academic Press, 2009.

Talairach, J., & Tournoux, P. (1988). *Co-planar stereotaxic atlas of the human brain*. Stuttgart: Georg Thieme Verlag.

Thiebaut de Schotten, M., ffytche, D. H., Bizzi, A., Dell'Acqua, F., Allin, M., Walshe, M., *et al.* (2011). Atlasing location, asymmetry and inter-subject variability of white matter tracts in the human brain with MR diffusion tractography. *NeuroImage*, *54*, 49–59. http://doi.org/10.1016/j.neuroimage.2010.07.055

Thiebaut de Schotten, M., Tomaiuolo, F., Aiello, M., Merola, S., Silvetti, M., Lecce, F., *et al.* (2014). Damage to white matter pathways in subacute and chronic spatial neglect: A group study and 2 single-case studies with complete virtual "in vivo" tractography dissection. *Cerebral Cortex*, *24*, 691–706. http://doi.org/10.1093/cercor/bhs351

Tuch, D. S., Reese, T. G., Wiegell, M. R., & Van J Wedeen. (2003). Diffusion MRI of complex neuralarchitecture.*Neuron*,*40*,885–895.http://doi.org/10.1016/S0896-6273(03)00758-X

Tuch, D. S., Reese, T. G., Wiegell, M. R., Makris, N., Belliveau, J. W., & Wedeen, V. J. (2002). High angular resolution diffusion imaging reveals intravoxel white matter fiber heterogeneity. *Magnetic Resonance in Medicine*, *48*, 577–582. http://doi.org/10.1002/mrm.10268

Van Essen, D. C. (1997). A tension-based theory of morphogenesis and compact wiring in the central nervous system. *Nature*, *385*, 313–318. http://doi.org/10.1038/385313a0

Wakana, S., Caprihan, A., Panzenboeck, M. M., Fallon, J. H., Perry, M., Gollub, R. L., *et al.* (2007). Reproducibility of quantitative tractography methods applied to cerebral white matter. *NeuroImage*, *36*, 630–644.

Wedeen, V. J., Hagmann, P., Tseng, W.-Y. I., Reese, T. G., & Weisskoff, R. M. (2005). Mapping complex tissue architecture with diffusion spectrum magnetic resonance imaging. *Magnetic Resonance in Medicine*, *54*, 1377–1386. http://doi.org/10.1002/mrm.20642

Wheeler-Kingshott, C. A. M., & Cercignani, M. (2009). About "axial" and "radial" diffusivities. *Magnetic Resonance in Medicine*, *61*, 1255–1260. http://doi.org/10.1002/mrm.21965

Further Reading and Resources

Catani, M., & Thiebaut de Schotten, M. (2012). *Atlas of human brain connections*. Oxford: Oxford University Press.

Damasio, H., & Damasio, A. (1989). *Lesion analysis in neuropsychology*. New York: Oxford University Press.

Johansen-Berg, H., & Behrens, T. E. J. (Eds.) (2013). *Diffusion MRI: From quantitative measurement to in vivo neuroanatomy*, 2nd ed. Academic Press: Elsevier.

Jones, D. (Ed.) (2010). *Diffusion MRI*. Oxford: Oxford University Press.

Stemme, B., & Whitacker, H. (Eds.) (2008). *Handbook of the neuroscience of language*. London: Elsevier Academic Press.

Toga, A. (Ed.) (2015). *Brain mapping: An encyclopedic reference*, 1st ed. Academic Press: Elsevier.